HHS Public Access

Author manuscript

*Lebensm Wiss Technol*. Author manuscript; available in PMC 2023 January 15.

Published in final edited form as:

*Lebensm Wiss Technol*. 2022 January 15; 154: . doi:10.1016/j.lwt.2021.112751.

# Nanoencapsulation of apigenin with whey protein isolate: physicochemical properties, *in vitro* activity against colorectal cancer cells, and bioavailability

**Shan Hong**[1,#], **Vermont P Dia**[1], **Seung Joon Baek**[2], **Qixin Zhong**[1,*]

[1]Department of Food Science, The University of Tennessee, Knoxville, TN, USA

[2]College of Veterinary Medicine, Seoul National University, Seoul 08826, South Korea

## Abstract

Incorporating lipophilic phytochemicals with anti-cancer activities in functional beverages requires an appropriate nanoencapsulation technology. The present objective was to encapsulate apigenin with whey protein isolate (WPI) utilizing a pH-cycle method and subsequently characterize physicochemical properties, the *in vitro* anticancer activities against human colorectal HCT-116 and HT-29 cancer cells, and the *in vivo* bioavailability. Up to 2.0 mg/mL of apigenin was nanoencapsulated with 1.0 mg/mL WPI, with an encapsulation efficiency of up to 98.15% and loading capacity of up to 196.21 mg/g-WPI. Nanodispersions were stable during storage, and apigenin became amorphous after encapsulation. Nanoencapsulation and *in vitro* digestion did not reduce the anti-proliferative activity of apigenin. Nanoencapsulation of apigenin enhanced the cellular uptake, the pro-apoptotic effects, and the bioavailability in the mice's blood and colon mucosa when comparing to the unencapsulated apigenin. Therefore, the present work may be significant to incorporate lipophilic phytochemicals in functional beverages for disease prevention.

### Keywords

apigenin; whey protein isolate; nanoencapsulation; *in vitro* anticancer activity; bioavailability

[*]Corresponding Author: Department of Food Science, The University of Tennessee, 2510 River Drive, Knoxville, TN 37996, United States, qzhong@utk.edu.

[#]Current address: Department of Grain Science and Industry, Kansas State University, 1301 Middle Campus Drive, 66506, USA. shanhong@ksu.edu

CRediT authorship contribution statement

**Shan Hong:** Data curation; Formal analysis; Investigation; Methodology; Software; Visualization; Roles/Writing - original draft; Writing - review & editing. **Vermont P Dia:** Investigation; Methodology; Writing - review & editing. **Seung Joon Baek:** Conceptualization; Writing - review & editing. **Qixin Zhong:** Conceptualization; Funding acquisition; Methodology; Project administration; Resources; Supervision; Writing - review & editing.

Declaration of interests

The authors declare that they have no known competing financial interests or personal relationships that could have appeared to influence the work reported in this paper.

## 1. Introduction

Polyphenols naturally occurring in plants are antioxidants with numerous biological activities (Archivio, Filesi, Di Benedetto, Gargiulo, Giovannini, & Masella, 2007; Scalbert, Johnson, & Saltmarsh, 2005) and have low toxicity at a physiologically relevant concentration (Xie, Yang, Zhou, Zhu, Lee, & Teng, 2016). Apigenin (4′,5,7-trihydroxyflavone) is abundant in fruits and vegetables such as celery, parsley, onions, and chamomile (Zhou, Wang, Zhou, Song, & Xie, 2017). Apigenin has a broad spectrum of health benefits resulting from its free radical scavenging and anti-inflammatory properties (Tian et al., 2021; Zhang, Wang, Gurley, & Zhou, 2014). With non-mutagenesis and relatively low toxicity, apigenin is a potential agent to develop strategies to prevent and cure cancers (Shukla & Gupta, 2010). Studies using human colon carcinoma cell lines have shown the activity of apigenin to inhibit cell proliferation (Xu, Wang, Song, Yao, Huang, & Zhu, 2016), promote cell cycle arrest (Gupta, Afaq, & Mukhtar, 2002), and induce cell apoptosis (Lee et al., 2014). However, the application of apigenin to improve human health is hampered by its low water solubility of 2.16 μg/mL at pH 7.5 (Zhang, Liu, Huang, Gao, & Qian, 2012). The low water solubility limits its incorporation in aqueous systems and the bioavailability. Another cause leading to the low *in vivo* bioavailability and therapeutic efficacy of apigenin is the rapid metabolism and elimination via glucuronidation and sulfation (Ali, Rahul, Naz, Jyoti, & Siddique, 2017). Therefore, much work is needed to enhance the solubility and bioavailability of apigenin.

Encapsulation of lipophilic polyphenols in nanoscale particulates has now been studied extensively to improve their solubility, bioavailability, and bioactivity. For apigenin, delivery systems have been studied by nanoencapsulation in distearoylphosphatidylcholine liposomes (Banerjee, Banerjee, Das, & Mandal, 2015), micelles of triblock polymers of poly(ethylene oxide)-poly(propylene oxide)-poly(ethylene oxide) and polyethylene glycol-660 hydroxystearate (Zhai et al., 2013), and nanoparticles of poly(lactic-co-glycolic acid) (Das, Das, Samadder, Paul, & Khuda-Bukhsh, 2013). Alternation of dimension and structure of apigenin has been studied for nanocrystals prepared by sequential bead milling and high-pressure homogenization (Al Shaal, Shegokar, & Müller, 2011) and sub-micron particles with amorphous apigenin after precipitation in supercritical carbon dioxide (Zhang, Huang, Liu, Gao, & Qian, 2013). Synthetic polymers, toxic organic solvents, and expensive processes are limitations in these studies, particularly for food applications.

An organic solvent-free technology was developed to encapsulate curcumin in sodium caseinate in our research group (Pan, Luo, Gan, Baek, & Zhong, 2014). The principle is based on a pH-cycle, by first increasing a neutral dispersion to pH 12.0 to deprotonate phenolic hydroxyl groups and thus dissolve a polyphenol to molecularly bind with caseinate, followed by gradually lowering pH to 7.0 during which polyphenols become protonated and precipitate together with bound caseinate to self-assemble as nanoscale particles of a diameter of 20–30 nm. The encapsulation was performed at room temperature on a magnetic stirring plate, and the nanoencapsulated curcumin was more effective against the proliferation of human colorectal HCT-116 and pancreatic BxPC3 cancer cells than curcumin dissolved in dimethyl sulfoxide (DMSO). The technology has been adapted to encapsulate various polyphenols using various biomolecular carriers. In preliminary

experiments, the same process to encapsulate apigenin using sodium caseinate resulted in dispersions that showed precipitation after overnight storage. With the combination of casein and hydrophobic rice protein, spherical nanocapsules with a dimension of 30–60 nm were prepared, and the nanoencapsuled apigenin effectively inhibited the tumor growth after intraperitoneal injection at 20 mg/kg body mass of mice (Wang, Chen, Zhong, Chen, Wang, & Patel, 2019).

Since dairy proteins are abundant, sustainable, and inexpensive, the first objective of the present study was to study the characteristics of the pH-cycle method encapsulating apigenin using another group of dairy proteins - whey protein isolate (WPI). The second objective was to characterize the *in vitro* activity of nanoencapsulated apigenin inhibiting the proliferation of human colorectal cancer cell lines (HCT-116 and HT-29) and the bioavailability in the blood and colon mucosa of mice.

## 2. Materials and methods

### 2.1. Materials

Apigenin (> 98% purity) was procured from Indofine Chemical Co. Inc (Hillsborough, NJ, USA). WPI was a kind gift provided by Hilmar Ingredients (Hilmar, CA, USA). Human colon HCT-116 and HT-29 cancer cell lines were ordered from American Type Culture Collection (Manassas, VA, USA). The minimum essential medium (MEM), 1X, was from Corning Inc. (Corning, New York, NY, USA). Fetal bovine serum (FBS) was ordered from Life Technologies (Carlsbad, CA, USA). Unless stated otherwise, other chemicals were products of Thermo Fisher Scientific (Pittsburgh, PA, USA).

### 2.2. Encapsulation of apigenin using WPI

Our previous pH-cycle method (Pan et al., 2014) was adopted to encapsulate apigenin in WPI at room temperature (RT, 21 °C), with some modifications. WPI was hydrated at 10.0 mg/mL in deionized water overnight at 4 °C. After adding apigenin at 0.6–2.0 mg/mL in the WPI solution, the mixture pH was adjusted to 13.0 using 2.0 mol/L KOH solution and stirred for 5 min. After adjusting to pH 10.0, the mixture was stirred for another 30 min before titration to pH 7.0 with 1.0 M HCl. Transparent dispersions were obtained after centrifuging samples at 10,000 *g* and 4 °C for 10 min (Sorvall LYNX 6000 Centrifuge, Thermo Fisher Scientific, Waltham, MA, USA). The dispersions were also lyophilized (Model Advantage Plus EL-85, VirTis Company, Inc., Gardiner, NY, USA) for characterization. The precipitate after centrifugation was dissolved with DMSO, and the absorbance at 337 nm was measured to quantify the unencapsulated apigenin based on a standard curve prepared with standard solutions with apigenin dissolved in DMSO. The encapsulation efficiency (EE) and loading capacity (LC) were then determined according to eqs. 1 and 2, respectively.

$$\mathrm{EE}\% = \frac{total\ apigenin\ (mg) - \ unencapsulated\ apigenin\ (mg)}{total\ apigenin\ (mg)} \times 100 \quad (1)$$

$$\mathrm{LC(mg/g)} = \frac{total\ apigenin\ (mg) - \ unencapsulated\ apigenin\ (mg)}{total\ WPI\ (g)} \quad (2)$$

## 2.3. Physicochemical properties of dispersions

**2.3.1. Particle size distribution and zeta-potential—**Dynamic light scattering (DLS) was used to determine particle size distributions of pH 7.0 dispersions during 30-day storage at RT. Dispersions were added with 0.2 mg/mL sodium azide to prevent microbial spoilage during storage. Both the particle size and zeta-potential measurements were performed with a Zetasizer Nano-ZS series instrument (Malvern Instruments, Ltd., Worcestershire, UK).

**2.3.2. Morphology—**Scanning transmission electron microscopy (STEM) was used to characterize the morphology of the dispersion prepared with 2.0 mg/mL apigenin. The dispersion was diluted by 100 times in deionized water, corresponding to a WPI concentration of 100 μg/mL. One drop of the diluted sample was placed on a freshly glow-discharged 400-mesh carbon copper grid coated with a thin carbon film. The sample was stained by placing the grid in a drop of 10.0 mg/mL uranyl acetate for 1 min and dried at RT. Images were collected using a Zeiss Auriga microscope (Carl Zeiss Microscopy, Oberkochen, Germany) at 30 kV.

**2.3.3. Thermal properties—**Differential scanning calorimetry (DSC) was used to characterize thermal properties of the powder lyophilized from the dispersion prepared with 2 mg/mL apigenin, lyophilized WPI treated at the pH-cycle conditions, and pristine apigenin using a model Q2000 calorimeter (TA Instruments, New Castle, DE, USA). Approximately 3 mg powder was used for each sample. After sealing in a hermetic aluminum pan, samples were heated from 20 to 400 °C and then cooled from 400 to 25 °C at 10 °C/min. Nitrogen was used at 50 mL/min as a purge gas (Sun, Gao, & Zhong, 2018).

**2.3.4. X-ray Diffraction—**The X-ray diffraction (XRD) patterns of pristine apigenin, unprocessed WPI, lyophilized WPI after the pH-cycle treatment, lyophilized nanodispersion prepared with 2 mg/mL apigenin, and a physical mixture of pristine apigenin and unprocessed WPI were characterized at a $2\theta$ range from 5° to 60° using an Empyrean 2 diffractometer (PANalytical Inc., Westborough, WA, USA) with Ni-filtered Cu Kα radiation. Measurements were performed at a voltage of 45 kV and 40 mA.

**2.3.5. Fourier transform infrared (FTIR) spectroscopy—**FTIR spectroscopy was used to study molecular interactions between apigenin and WPI (Sun et al., 2018). Freeze-dried samples were directly placed on the flat top-plate fitted with a ZnSe crystal of a Spectrum Two FT-IR spectrometer (Spectrum Spotlight, PerkinElmer Inc., Waltham, MA, USA) equipped with an attenuated total reflection cell. The FTIR spectra at a wavenumber range of 400–4000 $cm^{-1}$ and a resolution of 4 $cm^{-1}$ were generated from 64 scans of each sample.

### 2.4. Simulated gastrointestinal digestions

To perform simulated digestions, a literature method was applied after modifications (A. Wang, Leible, Lin, Weiss, & Zhong, 2020). Free apigenin was prepared at 20 mmol/L in DMSO. The nanodispersion prepared with 2.0 mg/mL apigenin was used. The 10.0 mg/mL WPI solution before or after treatment at the pH-cycle conditions was also compared. The simulated gastric fluid (SGF) was prepared with 1.5 mg/mL pepsin (≥ 250 units/mg solid) in 2 g/L NaCl solution at pH 2. The simulated intestinal fluid (SIF) was prepared with 5 mg/mL pancreatin (8 × USP specifications) and 5 mg/mL bile salt in 0.1 mol/L PBS (pH 7.0). Experimentally, 200 μL of free apigenin, 500 μL of the nanodispersion, or 500 μL of WPI solution was mixed with 6 mL of the SGF, and the mixtures were adjusted to pH 2.0 and incubated in a water bath shaker (New Brunswick Scientific Co Inc., Edison, NJ, USA) operating at 150 rpm and 37 °C for 2 h. Subsequently, the mixture was blended with 4 mL of the SIF and adjusted to pH 7.0 with 1.0 mol/L NaOH, followed by incubation in the above water bath shaker for 4 h and termination of digestion by heating at 75 °C for 20 min. At the end of 2-h digestion with the SGF and 4-h digestion with the SIF, 1 mL aliquots of each sample were withdrawn for gel electrophoresis. The samples after terminating the digestions were also used in cell culture studies.

### 2.5. Sodium dodecyl sulfate polyacrylamide gel electrophoresis (SDS-PAGE)

SDS-PAGE was used to analyze the molecular weight changes of dispersions with 10.0 mg/mL WPI before and after the pH-cycle treatment, after encapsulation with 2 mg/mL apigenin, and after simulated digestions. Each liquid sample was mixed with the same volume of a Laemmli buffer containing 50.0 mg/mL β-mercaptoethanol (Bio-Rad Laboratories, Inc., Hercules, CA, USA). After heating in boiling water for 5 min, samples with an equivalent amount of protein were analyzed using a 4–20% Mini-Protean TGX gel (Bio-Rad Laboratories, Inc., Hercules, CA, USA). After electrophoresis at 200 V for 30 min, gels were washed with deionized water twice for 10 min each and stained with Bio-SafeTM Coomassie G-250 blue dye, followed by destaining with deionized water.

### 2.6. Activity of apigenin inhibiting proliferation of colon cancer cells

The anti-proliferative activity of free and encapsulated apigenin before and after the simulated digestions was assessed for human colorectal HCT-116 and HT-29 cancer cells using the Cell Titer 96 Aqueous One Solution Cell Proliferation Assay (Promega, Madison, WI, USA). The cells were cultured in the MEM with 10 mL/100 mL heat-inactivated FBS and 1 mL/100 mL penicillin/streptomycin at 37 °C under a humidified atmosphere of 5% $CO_2$. Cells were seeded at a density of 1000 cells/well in 200 μL complete medium in 96-well plates and incubated overnight to allow attachment. The free apigenin dissolved in DMSO was filtered with a 0.22 μm polyvinylidene fluoride filter. Encapsulated apigenin and their digested counterparts were pasteurized at 70 °C for 30 min. Both free and encapsulated apigenin were diluted to 0–20 μmol/L with culture medium before being applied to treat cells. WPI processed under the same pH cycle treatment that was diluted to an amount identical to that of the encapsulated apigenin was also studied. After incubation for 72 h, the growth medium was removed, and 100 μL MEM containing 10 mL/100 mL 3-(4,5-dimethylthiazol-2-yl)-5-(3-carboxymethoxyphenyl-2-(4-sulfophenyl)-2H-tetrazolium

inner salt (MTS) was added. Following incubation at 37 °C for 3 h, the absorbance at 490 nm was measured, and the growth inhibitory activity was calculated as the percentage of the absorbance of treatment wells with respect to that of the untreated control. For each of the sample triplicates, at least four cell replicates were used.

### 2.7. Cellular uptake of apigenin

The uptake of free and encapsulated apigenin by colon cancer cells was determined by modifying our previous method (Chen, Guan, Baek, & Zhong, 2019). Free and encapsulated apigenin was prepared as in the above simulated digestion section and diluted to 5, 10, and 20 μmol/L with the growth medium. Cancer cells seeded at $2 \times 10^5$ per well in 6-well plates were incubated overnight at 37 °C for attachment, followed by apigenin treatment for 24 h. The treatment cells were washed two times with cold PBS, lysed, and harvested with a radio immunoprecipitation assay buffer dissolved with 1 mL/100mL protease inhibitor cocktail. After vortexing the lysate at 4 °C for 5 min, 5 μL aliquots of the lysate were determined for the protein concentration using the Bradford assay with bovine serum albumin being the standard. The remaining lysate was added with two volumes of methanol, vortexed at 4 °C for 10 min, and sonicated for 30 min at 4 °C (Branson 1510 Ultrasonic Cleaner, MO, USA). Following centrifugation at 13,800 *g* and 4 °C for 10 min (Sorvall Legend Micro 21R Microcentrifuge, Thermo Fisher Scientific, Waltham, MA, USA), the supernatant was analyzed for the apigenin concentration using a reversed phase high performance liquid chromatography (HPLC) system (1200 series, Agilent Technologies, Waldbronn, Germany) equipped with an Agilent ZORBAX Eclipse Plus C18 HPLC column (150 mm × 4.6 mm, 5 μm, Agilent, Palo Alto, CA, USA), with the UV detector set at 340 nm. The mobile phase gradient was run from a binary mixture with 88:12 volume ratio of 40.0 mg/mL formic acid in water and acetonitrile to the same solution mixture at a volume ratio of 50:50. Standard solutions with 0–2.5 μg/mL apigenin dissolved in DMSO were used to establish a standard curve ($y = 76.262\ x$, $R^2 = 0.9997$). The cellular uptake of apigenin was then calculated according to eq. 3.

$$\text{Uptake of AP}(\mu\text{ g/mg}) = \frac{C_{\text{AP}}(\mu\text{ g/mL})}{C_{\text{P}}(\text{mg/mL})} \tag{3}$$

Where, $C_{\text{AP}}$ and $C_{\text{P}}$ are the respective concentrations of apigenin and protein in the cell lysate.

### 2.8. Cell cycle analysis using flow cytometry

Flow cytometry was used to analyze the cell-cycle distribution and the apoptotic ratio as interfered by free or encapsulated apigenin. Cells were prepared and treated with 5, 10, and 20 μmol/L for 24 h, as detailed in the cellular uptake section, and were collected with trypsinization. The harvested cells were centrifuged at 1,000 *g* and 4 °C for 5 min, and the pellet was collected, re-suspended in 60 μL cold PBS, and fixed in 1 mL of ice-cold 70 mL/100mL ethanol. Following incubation overnight at 4 °C, the samples were centrifuged at 1,000 *g* and 4 °C for 10 min (Sorvall Legend Micro 21R Microcentrifuge, Thermo Fisher Scientific, Waltham, MA, USA) to collect the permeabilized cells that were then re-suspended in 1 mL PBS containing 16 μg/mL propidium iodide (PI) and 30 μg/mL

RNase A. Following incubation at 37 °C for 60 min in the dark, the fluorescence intensity was determined at an excitation wavelength of 488 nm using a flow cytometer (model using MACSQuant, Miltenyi Biotec Inc., Bergisch Gladbach, Germany). Each sample was acquired for a total of 10,000 events, and the results were reported for the percentage of cells in each phase of the cell cycle. Three independent replicates were analyzed.

## 2.9. Bioavailability of apigenin

**2.9.1. Animals and sample preparation—**Animal experiments followed the Protocol #2369–0615 approved by the University of Tennessee Animal Care and Use Committee, in compliance with the National Institutes of Health guidelines for the care and use of laboratory animals. Thirty 7-week-old C57BL/6J mice (strain for $Apc^{Min+}$ mice), including both males and females, were ordered from Jackson Laboratories (Harbor, ME, USA) and were randomly placed in standard mouse cages and provided with rodent diet and water *ad libitum*. The animal facility was maintained at 23 ± 2 °C, 30–70% relative humidity, and a cycle of 12 h light and 12 h dark. After random separation into two groups after one week of acclimatization, mice were orally gavaged with free apigenin, prepared by suspending pristine apigenin in 5.0 mg/mL methylcellulose (vehicle) at 6.3 mg/mL, or encapsulated apigenin prepared with 40.0 mg/mL WPI and 8 mg/mL apigenin that was diluted to 6.3 mg/mL apigenin with deionized water and pasteurized by heating at 75 °C for 20 s, at a dosage of 50 mg/kg body mass. Following euthanization with $CO_2$ inhalation at about 0, 1, 6, and 24 h after gavaging, blood was taken by cardiac puncture, and colon mucosa was collected and stored in ice-cold PBS at 4 °C. The serum collected after centrifuging blood samples at 900 *g* for 15 min (Sorvall Legend Micro 21R Microcentrifuge, Thermo Fisher Scientific, Waltham, MA, USA) was stored at −80 °C.

**2.9.2. Measurement of apigenin in mouse colon mucosa and blood serum—**Samples stored at −80 °C were thawed at 4 °C overnight. Apigenin in the blood serum was extracted by mixing 50 μL of a serum sample with 100 μL of methanol (Wu et al., 2017). Following vortexing at 4 °C for 3 min and sonication at 4 °C for 20 min (Branson 1510 Ultrasonic Cleaner, St. Louis, MO, USA), the mixture was centrifuged at 13,800 *g* and 4 °C for 10 min (Sorvall Legend Micro 21R Microcentrifuge, Thermo Fisher Scientific, Waltham, MA, USA) to obtain the supernatant for HPLC quantification using the above protocol.

The colon mucosa sample was rinsed with PBS, added with 3 mL of clean PBS, and homogenized twice for 30 s each at 8,000 rpm (Kinematica Polytron PT 10/35 GT Homogenizer, Fisher Scientific, Hampton, NH, USA). Following centrifugation at 1,900 *g* and 4 °C for 10 min (Sorvall Legend Micro 21R Microcentrifuge, Thermo Fisher Scientific, Waltham, MA, USA), the supernatant was transferred and extracted for apigenin following the same procedures as those of mice serum samples. The precipitate after centrifugation was added with 1 mL of DMSO, vortexed at the ambient temperature for 1 h, and centrifuged for 10 min at 14,000 *g* (Sorvall Legend Micro 21R Microcentrifuge, Thermo Fisher Scientific, Waltham, MA, USA). The supernatant was then used in the HPLC quantification of apigenin as detailed previously.

### 2.10. Statistical analysis

Results were reported for mean ± SD and data were analyzed with one-way ANOVA using the IBM SPSS Statistics version 25.0 software (SPSS Inc., Chicago, IL, USA). The Tukey test was applied for multiple comparisons at a significance level of 0.05.

## 3. Results and discussion

### 3.1. Physicochemical properties of apigenin encapsulated in WPI

**3.1.1. Encapsulation properties—**For WPI-apigenin mixtures after the pH-cycle treatment, the EE increased from 93.22% to 98.15%, and the corresponding LC increased from 57.19 to 196.21 mg-apigenin/g-WPI when the apigenin content in the mixture increased from 0.6 to 2.0 mg/mL (Figure 1A). The EE and LC are higher than previous studies encapsulating apigenin in liposomes and polymeric micelles (Banerjee et al., 2015; Zhai et al., 2013), possibly because of the molecular binding between apigenin and whey proteins during the pH-cycle. The pH-cycle method with varied alkaline pH and incubation time has been widely applied to form protein-based nanoparticles with and without lipophilic bioactive compounds, including NaCas-zein-propylene glycol alginate (Sun et al., 2018), zein/tea saponin/curcumin (Yuan, Xiao, Zhang, Ma, Wang, & Xu, 2021), and casein/rice protein/apigenin (Wang et al., 2019) composite nanoparticles. A lower LC and a lower EE than the present study were observed previously when mixtures with 20.0 mg/mL sodium caseinate and 0.2–2.0 mg/mL curcumin were processed with the pH-cycle (Pan et al., 2014). Major components of WPI, β-lactoglobulin and α-lactalbumin, have a large portion of hydrophilic amino acid residues on the surface to remain highly soluble at the corresponding pI (Damodaran & Parkin, 2017), which is different from the isoelectric precipitation of caseins. At alkaline pH, whey proteins are unfolded to expose hydrophobic amino acid residues to bind with deprotonated apigenin (W. Chen et al., 2019). During the subsequent neutralization to pH 7, the denatured whey proteins are refolded, and apigenin becomes insoluble to attract apigenin bound to other whey proteins, forming capsules with an apigenin core and a whey protein shell. In contrast, caseins have distinct hydrophobic and hydrophilic segments on the primary structure and have few secondary and tertiary structures. The casein-curcumin capsules formed during the neutralization step of the pH-cycle can have a more hydrophobic surface than those of WPI, more significant at a higher content of curcumin. Additionally, curcumin is more hydrophobic than apigenin, as suggested by its lower water solubility (0.6 μg/mL (Kurien, Singh, Matsumoto, & Scofield, 2007) vs. 2.16 μg/mL (Zhang et al., 2012)). Removal of bigger capsules after centrifugation may have resulted in a lower EE of curcumin in the previous study. A much lower EE and LC than the current study were also reported when curcumin was loaded in WPI-zein composite nanocapsules (Zhan, Dai, Zhang, & Gao, 2020). Nevertheless, a high LC is desired in developing delivery systems (S. Wang et al., 2014).

**3.1.2. Dimension, structure, stability, and interactions—**The Z-average diameter of dispersions increased from 180 to 240 nm when the amount of apigenin used in encapsulation increased. This is expected due to the increase in LC (Figure 1A). Well dispersed, mostly spherical particles with a dimension of 200–400 nm were observed in the STEM for the dispersion with 2 mg/mL apigenin (Figure 1B), which agreed with the

DLS results. During ambient storage for 30 days, the size distribution of nanodispersions prepared with different amounts of apigenin remained unchanged (Figure 1C), indicating the absence of aggregation. The zeta-potential of nanodispersions was similar to that of WPI after the same pH cycle treatment (Table 1), which suggests the above mentioned unfolding and refolding of whey proteins during the pH cycle to form nanocapsules with surface characteristics similar to those of whey proteins. All dispersions had a similar zeta-potential magnitude of around 20 mV at pH 7.0 ($p > 0.05$) (Liu & Zhong, 2013). For colloidal particles, electrostatic repulsion is considered to be strong enough to prevent aggregation at a zeta-potential magnitude of ~25 mV (Shnoudeh et al., 2019). It is possible the hydrophilic surface of nanocapsules additionally contributed to the storage stability, similar to whey proteins at an acidity near pI (Damodaran et al., 2017). Because the nanodispersion prepared with 2 mg/mL apigenin had the highest LC and was stable during storage, this treatment was used for the rest of this study.

The DSC thermal properties are presented in Figure 2A. The pristine apigenin had a sharp endothermic peak at 366 °C, which is close to the melting point of 360.82 °C measured for apigenin crystals (Telange, Patil, Pethe, Fegade, Anand, & Dave, 2017). In contrast, the lyophilized capsules had a similar thermogram as WPI, without the endothermic melting peak of pristine apigenin. The lack of melting characteristics of capsules in DSC indicates the amorphous structure of apigenin in the capsules (Pan et al., 2014), which was further verified in XRD (Figure 2B). The XRD pattern of pristine apigenin exhibited several characteristic peaks, indicating its crystalline state. The physical mixture of pristine apigenin and unprocessed WPI displayed similar intense crystalline peaks. In contrast, the XRD pattern of nanocapsules was similar to that of WPI after the pH-cycle treatment, with the absence of peaks characteristic of apigenin crystals, suggesting the amorphous structure of apigenin when entrapped in the protein matrix (Pan, Zhong, & Baek, 2013; Wu et al., 2017). The sharp peaks in the XRD patterns of nanocapsules and WPI were contributed by KCl crystals used in pH adjustment (HCl and KOH). The amorphous structure after transforming phytochemical crystals increases the solubility and bioaccessibility (Wang et al., 2020).

The potential molecular interactions between apigenin and WPI were studied with FTIR, shown in Figure 2C. All samples had an absorption peak at around 3277–3282 $cm^{-1}$ that can be assigned to hydroxy stretching vibration (O-H) associated with intermolecular hydrogen bonds (Jiang, Li, Chai, & Leng, 2010). The bands at the 1700–1500 $cm^{-1}$ are attributed to the amide I (1700–1600 $cm^{-1}$) and amide II (1600–1500 $cm^{-1}$) bonds of proteins (Jiang et al., 2010). The absorption peak of pristine apigenin at 1652 $cm^{-1}$ shifted to 1631 $cm^{-1}$ after encapsulation, indicating the physical binding between apigenin and whey proteins. The absorbance peak at 1520 $cm^{-1}$ of unprocessed WPI shifted to 1531 $cm^{-1}$ and 1532 $cm^{-1}$ for WPI after the pH-cycle treatment and after encapsulating apigenin, respectively, which indicates the role of hydrophobic interactions involved in refolding whey proteins and self-assembling to form nanocapsules. The FTIR results suggest that physical interactions were involved in formation of nanocapsules. The absence of covalent bond formation and protein hydrolysis during the pH-cycle treatment was confirmed for the same SDS-PAGE profile of unprocessed WPI, WPI after the pH-cycle treatment, and the nanodispersion (Figure 3).

### 3.2. *In vitro* anti-proliferative activity of free and nanoencapsulated apigenin

Since uncontrolled cell proliferation is a hallmark of cancers, the ability of free (pre-dissolved in DMSO) and nanoencapsulated apigenin to inhibit the proliferation of human colorectal HCT-116 and HT-29 cancer cells was determined, presented in Figure 4. Treatments with 5 μmol/L apigenin showed a similar inhibitory activity as the control cells ($p > 0.05$). Overall, greater inhibition was observed at a higher level of apigenin, and no significant difference between free and nanoencapsulated apigenin was observed at levels of 5 and 10 μmol/L ($p > 0.05$). At 20 μmol/L, nanoencapsulated apigenin inhibited the proliferation of cancer cells less effectively than free apigenin ($p < 0.05$): 29.62% vs. 48.21% for HCT-116 cells and 37.70% vs. 51.73% for HT-29 cells after 72 h incubation at 37 °C. WPI alone at a concentration identical to that of the nanoencapsulated apigenin treatments did not exert a significant effect on cell viability. The anti-proliferative activity, therefore, resulted from the nanoencapsulated apigenin.

Numerous studies have examined the potential of polyphenols as anti-cancer agents and the impact of nanoencapsulation on anti-cancer activity. Both improved and reduced activities of curcumin after nanoencapsulation have been reported for *in vitro* and *in vivo* studies against colon cancer, and the discrepancies can be attributed to different cell lines, animals, doses, treatment times, and encapsulation systems (Wong, Ngai, Chan, Lee, Goh, & Chuah, 2019). Relevant to food applications and the present study, curcumin nanoencapsulated in sodium caseinate following the pH-cycle had the improved activity than free curcumin in inhibiting the proliferation of human colorectal HCT-116 and pancreatic BxPC3 cancer cells (Pan et al., 2014), while the opposite was observed for curcumin nanoencapsulated in soluble soybean polysaccharide using the same encapsulation method (Pan, Chen, Baek, & Zhong, 2018). Encapsulation of caffeic acid phenethyl ester in skim milk powder microcapsules (Wang et al., 2020), sugar fatty acid ester nanocapsules (Guan, Chen, & Zhong, 2019), or microemulsions (H. Chen et al., 2019) also improved the anti-proliferation activity against HCT-116 cells at 20 μg/mL. Curcumin loaded in emulsomes (solid lipid nanoparticles coated with multi-layers of phospholipids) was less effective than free curcumin in inhibiting HCT-116 cells at a level of 2.5–50 μmol/L (Bolat, Islek, Demir, Yilmaz, Sahin, & Ucisik, 2020). Curcumin encapsulated in whey proteins was also reported to be more active than plain curcumin in inhibiting the growth of colon cancer SW480 cells (Jayaprakasha, Murthy, & Patil, 2016). Factors leading to the anti-proliferation activity of nanoencapsulated polyphenols likely include the solubility, the release characteristics, the uptake by cancer cells, and the binding at the target sites. Unfortunately, it is impossible to compare different studies conducted at varying conditions and methodologies.

Samples after *in vitro* digestions were further investigated for anti-proliferative activity at 10 and 20 μmol/L apigenin, shown in Figure 4. The *in vitro* digestions did not significantly impact the cytotoxicity of free apigenin at 10 and 20 μmol/L and nanoencapsulated apigenin at 10 μmol/L, while a significant increase in activity was observed for 20 μmol/L nanoencapsulated apigenin after digestions ($p < 0.05$). For digested WPI at concentrations comparable to the nanoencapsulation treatments, significant inhibition of cell proliferation was observed only at the highest level for HCT-116 (Figure 4A). Although protein hydrolysates were produced after the digestions (Figure 3) and peptides could

have anti-proliferative activities, WPI shall not be the cause of increasing the activity of nanoencapsulated apigenin after the simulated digestions for both cancer cells (Figure 4). Bile salt micelles may be more effective in dissolving the encapsulated apigenin to improve the activity observed in Figure 4. Nevertheless, the simulated digestions did not negatively affect the anti-proliferative activity of free and nanoencapsulated apigenin ($p < 0.05$).

### 3.3. Cellular uptake of apigenin

Cellular uptake of apigenin pre-dissolved in DMSO (free) and nanoencapsulated in whey proteins is presented in Figure 5. A higher intracellular apigenin concentration was observed at a higher dose of apigenin, and the significantly higher uptake of nanoencapsulated apigenin than free apigenin was only observed at 20 μmol/L in HCT-116, but at all treatment concentrations in HT-29. The increased cellular uptake of nanoencapsulated apigenin did not increase the anti-proliferative activity when compared to free apigenin (Figure 4). This is different from a previous study that showed both the increased cellular uptake and the enhanced anti-proliferative activity of caffeic acid phenethyl ester dissolved in microemulsions than that dissolved in DMSO (H. Chen et al., 2019). It may be due to the interaction between apigenin and its targets is not as effective when encapsulated in globular whey proteins. Additionally, the cellular uptake was mostly higher for HCT-116 than HT-29 cells, indicating differences in their cellular structures.

### 3.4. Effects of apigenin on cell cycle distribution

To identify the possible mechanisms involved in cell growth inhibited by apigenin, cell cycle distribution was evaluated using flow cytometry after free and nanoencapsulated apigenin treatments. Figure 6 shows an increase in the sub-G1 population of HCT-116 cells after 24 h treatment, indicating increase of apoptotic cells. Incubation with 20 μmol/L of free and nanoencapsulated apigenin significantly increased the sub-G1 cells, resulting in 2.69 and 3.27 folds that of control cells, respectively. The increase was consistent with the reduction of cells in other phases. Similar cell cycle profiles were also observed in HT-29 cells (Figure 7), showing 2.25 and 3.29 folds of apoptotic cells at the dose of 20 μmol/L free and nanoencapsulated apigenin, respectively, when compared to untreated cells. WPI alone did not significantly alter the cell cycle distribution (data not shown). These results indicate that apigenin affects cell proliferation at least in part by inducing apoptosis. Likewise, the nanoencapsulation can potentially induce apoptosis in these cells.

### 3.5. *In vivo* bioavailability of apigenin influenced by nanoencapsulation

The apigenin concentration in mice's blood serum and colon mucosa is shown in Figure 8. Overall, nanoencapsulation improved the bioavailability of apigenin. The maximum apigenin concentration in the serum reached 28.70 and 19.05 μmol/L one hour after gavage for nanoencapsulated and free apigenin, respectively (Figure 8A). After 6 h of oral gavage, apigenin in the mice colon accumulated to a level of 25.97 μg and 18.90 μg for nanoencapsulated and free apigenin, respectively (Figure 8B). The area-under-curve of the nanoencapsulated apigenin was 1.39 and 1.41 times that of free apigenin in the blood serum and colon mucosa, respectively. Nanoencapsulation facilitates the dissolving of lipophilic compounds in bile salt micelles to enhance the absorption into the blood (Lamsen, Wang, D'Souza, Dia, Chen, & Zhong, 2020), and the unabsorbed apigenin dissolved in nanoscale

bile salt micelles when passing into the colon can likely diffuse more effectively into the colon mucosa.

## 4. Conclusions

In the present study, high EEs of 93.22–98.15% and LCs of 57.19–196.21 mg-apigenin/g-WPI were achieved using WPI and the pH-cycle technology. The nanocapsules had hydrodynamic diameters of 180–240 nm and exhibited good storage stability. The improved dispersibility and small dimension of nanoencapsulated apigenin enhanced the uptake by human colon HCT-116 and HT-29 cancer cells. Nanoencapsulation significantly enhanced the cell cycle arrest in the sub-G1 phase, potentially inducing cell apoptosis, which partially contributed to the growth inhibitory activity of apigenin against cancer cells. Consistently, nanoencapsulation improved the bioavailability of apigenin in the mice's blood serum and colon mucosa. These findings may assist the development of functional beverages for disease prevention.

## Acknowledgments

Research reported in this publication was financially supported by the National Institute of Biomedical Imaging and Bioengineering of the National Institutes of Health, United States under award number a1R21EB018937–01A1, the University of Tennessee Institute of Agriculture, and the United States Department of Agriculture National Institute of Food and Agriculture Hatch Project TEN00568. Any opinions, findings, conclusions, or recommendations expressed in this publication are those of the author(s) and do not necessarily reflect the view of the funding agencies.

## References

Al Shaal L, Shegokar R, & Müller RH (2011). Production and characterization of antioxidant apigenin nanocrystals as a novel UV skin protective formulation. International journal of pharmaceutics, 420(1), 133–140. [PubMed: 21871547]

Ali F, Rahul, Naz F, Jyoti S, & Siddique YH (2017). Health functionality of apigenin: A review. International Journal of Food Properties, 20(6), 1197–1238.

Banerjee K, Banerjee S, Das S, & Mandal M (2015). Probing the potential of apigenin liposomes in enhancing bacterial membrane perturbation and integrity loss. Journal of colloid and interface science, 453, 48–59. [PubMed: 25965432]

Bolat ZB, Islek Z, Demir BN, Yilmaz EN, Sahin F, & Ucisik MH (2020). Curcumin- and piperine-loaded emulsomes as combinational treatment approach enhance the anticancer activity of curcumin on HCT116 colorectal cancer model. Frontiers in bioengineering and biotechnology, 8, 50. [PubMed: 32117930]

Chen H, Guan Y, Baek SJ, & Zhong Q (2019). Caffeic acid phenethyl ester loaded in microemulsions: Enhanced in vitro activity against colon and breast cancer cells and possible cellular mechanisms. Food Biophysics, 14(1), 80–89.

Chen W, Wang W, Ma X, Lv R, Watharkar RB, Ding T, … Liu D (2019). Effect of pH-shifting treatment on structural and functional properties of whey protein isolate and its interaction with (−)-epigallocatechin-3-gallate. Food Chem, 274, 234–241. [PubMed: 30372932]

D Archivio M, Filesi C, Di Benedetto R, Gargiulo R, Giovannini C, & Masella R (2007). Polyphenols, dietary sources and bioavailability. Annali Dell'Istituto Superiore Di Sanita, 43(4), 348.

Damodaran S, & Parkin KL (2017). Amino acids, peptides, and proteins. In Fennema's food chemistry (pp. 235–356): CRC Press.

Das S, Das J, Samadder A, Paul A, & Khuda-Bukhsh AR (2013). Efficacy of PLGA-loaded apigenin nanoparticles in Benzo [a] pyrene and ultraviolet-B induced skin cancer of mice: Mitochondria

mediated apoptotic signalling cascades. Food and chemical toxicology, 62, 670–680. [PubMed: 24120900]

Guan Y, Chen H, & Zhong Q (2019). Nanoencapsulation of caffeic acid phenethyl ester in sucrose fatty acid esters to improve activities against cancer cells. Journal of Food Engineering, 246, 125–133.

Gupta S, Afaq F, & Mukhtar H (2002). Involvement of nuclear factor-kappa B, Bax and Bcl-2 in induction of cell cycle arrest and apoptosis by apigenin in human prostate carcinoma cells. Oncogene, 21(23), 3727–3738. [PubMed: 12032841]

Jayaprakasha GK, Murthy KNC, & Patil BS (2016). Enhanced colon cancer chemoprevention of curcumin by nanoencapsulation with whey protein. European journal of pharmacology, 789, 291–300. [PubMed: 27404761]

Jiang Y, Li Y, Chai Z, & Leng X (2010). Study of the physical properties of whey protein isolate and gelatin composite films. J Agric Food Chem, 58(8), 5100–5108. [PubMed: 20356044]

Kurien BT, Singh A, Matsumoto H, & Scofield RH (2007). Improving the solubility and pharmacological efficacy of curcumin by heat treatment. Assay and drug development technologies, 5(4), 567–576. [PubMed: 17767425]

Lamsen MRL, Wang T, D'Souza D, Dia V, Chen G, & Zhong Q (2020). Encapsulation of vitamin D3 in gum arabic to enhance bioavailability and stability for beverage applications. Journal of food science, 85(8), 2368–2379. [PubMed: 32691454]

Lee Y, Sung B, Kang YJ, Kim DH, Jang J-Y, Hwang SY, … Chung HY (2014). Apigenin-induced apoptosis is enhanced by inhibition of autophagy formation in HCT116 human colon cancer cells. International journal of oncology, 44(5), 1599–1606. [PubMed: 24626522]

Liu G, & Zhong Q (2013). Thermal aggregation properties of whey protein glycated with various saccharides. Food Hydrocolloids, 32(1), 87–96.

Pan K, Chen H, Baek SJ, & Zhong Q (2018). Self-assembled curcumin-soluble soybean polysaccharide nanoparticles: Physicochemical properties and in vitro anti-proliferation activity against cancer cells. Food Chem, 246, 82–89. [PubMed: 29291882]

Pan K, Luo Y, Gan Y, Baek SJ, & Zhong Q (2014). pH-driven encapsulation of curcumin in self-assembled casein nanoparticles for enhanced dispersibility and bioactivity. Soft Matter, 10(35), 6820–6830. [PubMed: 25082426]

Pan K, Zhong Q, & Baek SJ (2013). Enhanced dispersibility and bioactivity of curcumin by encapsulation in casein nanocapsules. J Agric Food Chem, 61(25), 6036–6043. [PubMed: 23734864]

Scalbert A, Johnson IT, & Saltmarsh M (2005). Polyphenols: antioxidants and beyond. The American journal of clinical nutrition, 81(1), 215S–217S.

Shnoudeh AJ, Hamad I, Abdo RW, Qadumii L, Jaber AY, Surchi HS, & Alkelany SZ (2019). Synthesis, characterization, and applications of metal nanoparticles. In Biomaterials and bionanotechnology (pp. 527–612): Elsevier.

Shukla S, & Gupta S (2010). Apigenin: a promising molecule for cancer prevention. Pharmaceutical research, 27(6), 962–978. [PubMed: 20306120]

Sun C, Gao Y, & Zhong Q (2018). Properties of ternary biopolymer nanocomplexes of zein, sodium caseinate, and propylene glycol alginate and their functions of stabilizing high internal phase Pickering emulsions. Langmuir, 34(31), 9215–9227. [PubMed: 29979599]

Telange DR, Patil AT, Pethe AM, Fegade H, Anand S, & Dave VS (2017). Formulation and characterization of an apigenin-phospholipid phytosome (APLC) for improved solubility, in vivo bioavailability, and antioxidant potential. European Journal of Pharmaceutical Sciences, 108, 36–49. [PubMed: 27939619]

Tian C, Liu X, Chang Y, Wang R, Lv T, Cui C, & Liu M (2021). Investigation of the anti-inflammatory and antioxidant activities of luteolin, kaempferol, apigenin and quercetin. South African Journal of Botany, 137, 257–264.

Wang A, Leible M, Lin J, Weiss J, & Zhong Q (2020). Caffeic Acid Phenethyl Ester Loaded in Skim Milk Microcapsules: Physicochemical Properties and Enhanced In Vitro Bioaccessibility and Bioactivity against Colon Cancer Cells. J Agric Food Chem, 68(50), 14978–14987. [PubMed: 33140648]

Wang S, Su R, Nie S, Sun M, Zhang J, Wu D, & Moustaid-Moussa N (2014). Application of nanotechnology in improving bioavailability and bioactivity of diet-derived phytochemicals. The Journal of nutritional biochemistry, 25(4), 363–376. [PubMed: 24406273]

Wang T, Chen X, Zhong Q, Chen Z, Wang R, & Patel AR (2019). Facile and efficient construction of water-soluble biomaterials with tunable mesoscopic structures using all-natural edible proteins. Advanced Functional Materials, 29(31), 1901830.

Wong KE, Ngai SC, Chan K-G, Lee L-H, Goh B-H, & Chuah L-H (2019). Curcumin nanoformulations for colorectal cancer: a review. Frontiers in pharmacology, 10, 152. [PubMed: 30890933]

Wu W, Zu Y, Wang L, Wang L, Wang H, Li Y, … Fu Y (2017). Preparation, characterization and antitumor activity evaluation of apigenin nanoparticles by the liquid antisolvent precipitation technique. Drug delivery, 24(1), 1713–1720. [PubMed: 29115900]

Xie J, Yang Z, Zhou C, Zhu J, Lee RJ, & Teng L (2016). Nanotechnology for the delivery of phytochemicals in cancer therapy. Biotechnology advances, 34(4), 343–353. [PubMed: 27071534]

Xu M, Wang S, Song Y, Yao J, Huang K, & Zhu X (2016). Apigenin suppresses colorectal cancer cell proliferation, migration and invasion via inhibition of the Wnt/β-catenin signaling pathway. Oncology letters, 11(5), 3075–3080. [PubMed: 27123066]

Yuan Y, Xiao J, Zhang P, Ma M, Wang D, & Xu Y (2021). Development of pH-driven zein/tea saponin composite nanoparticles for encapsulation and oral delivery of curcumin. Food Chem, 364, 130401. [PubMed: 34174648]

Zhai Y, Guo S, Liu C, Yang C, Dou J, Li L, & Zhai G (2013). Preparation and in vitro evaluation of apigenin-loaded polymeric micelles. Colloids and Surfaces A: Physicochemical and Engineering Aspects, 429, 24–30.

Zhan X, Dai L, Zhang L, & Gao Y (2020). Entrapment of curcumin in whey protein isolate and zein composite nanoparticles using pH-driven method. Food Hydrocolloids, 106, 105839.

Zhang J, Huang Y, Liu D, Gao Y, & Qian S (2013). Preparation of apigenin nanocrystals using supercritical antisolvent process for dissolution and bioavailability enhancement. European Journal of Pharmaceutical Sciences, 48(4–5), 740–747. [PubMed: 23305994]

Zhang J, Liu D, Huang Y, Gao Y, & Qian S (2012). Biopharmaceutics classification and intestinal absorption study of apigenin. International journal of pharmaceutics, 436(1–2), 311–317. [PubMed: 22796171]

Zhang X, Wang G, Gurley EC, & Zhou H (2014). Flavonoid apigenin inhibits lipopolysaccharide-induced inflammatory response through multiple mechanisms in macrophages. PloS one, 9(9), e107072. [PubMed: 25192391]

Zhou X, Wang F, Zhou R, Song X, & Xie M (2017). Apigenin: A current review on its beneficial biological activities. Journal of Food Biochemistry, 41(4), e12376.

**Highlights:**

- Apigenin was encapsulated with whey protein isolate using a pH-cycle method.
- The encapsulation efficiency was up to 98.15% and the loading capacity was up to 196.21 mg/g-WPI.
- Nanodispersions were stable during 30-day storage at room temperature.
- Nanoencapsulation enhanced the apigenin uptake by and apoptosis of colon cancer cells.
- Nanoencapsulation enhanced apigenin bioavailability in mice’s blood and colon mucosa.

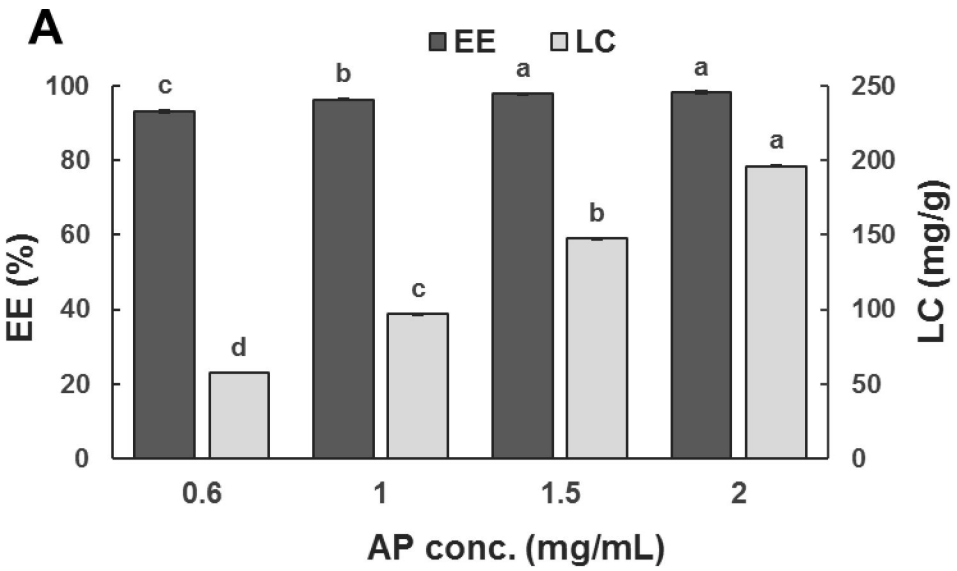


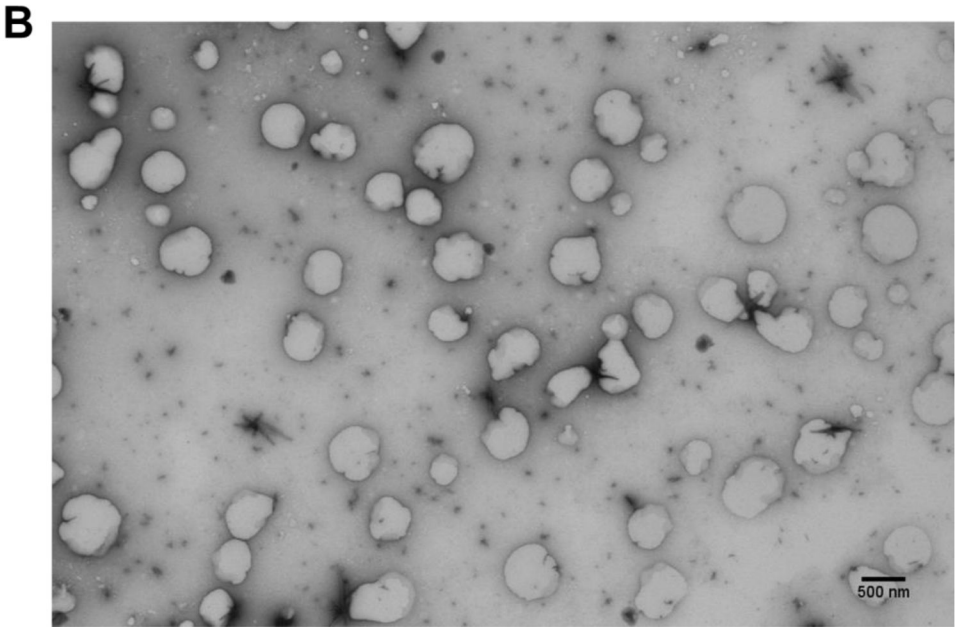

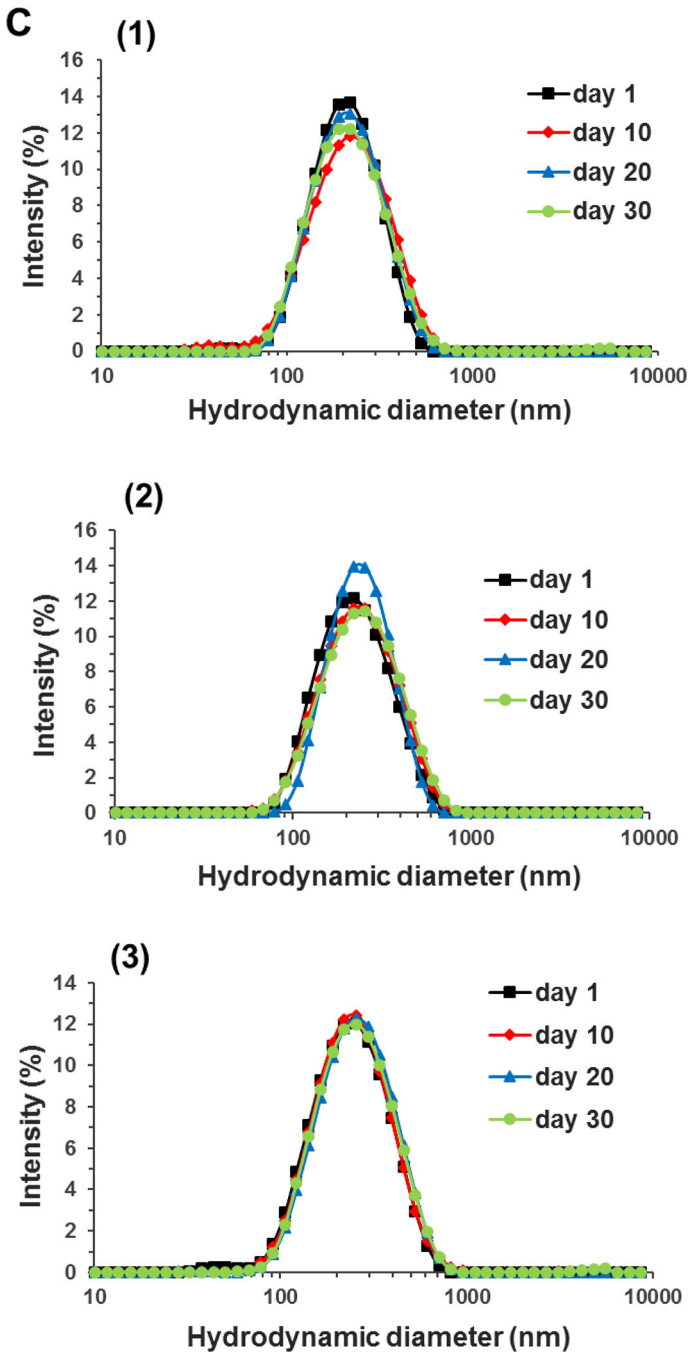

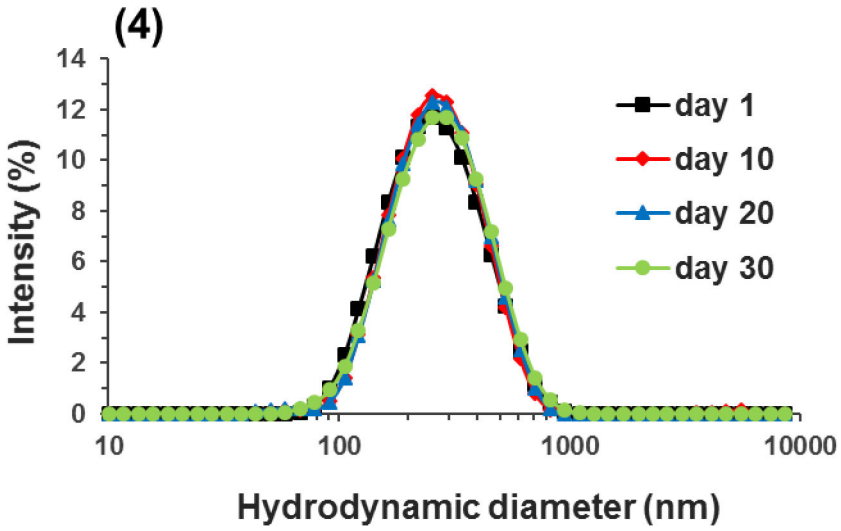


**Figure 1.**

(A) Encapsulation efficiency (EE%) and loading capacity (LC, mg/g-WPI) of mixtures with 10.0 mg/mL WPI and 0.6–2.0 mg/mL apigenin (AP) after the pH-cycle treatment; (B) STEM image of the nanodispersion prepared with 2.0 mg/mL AP in 10.0 mg/mL WPI; (C) Size distributions of pH 7.0 nanodispersions prepared with (1) 0.6, (2) 1.0, (3) 1.5, or (4) 2.0 mg/mL AP during 30-day storage at 21 °C. Error bars are SD (n = 3). Different letters above columns in (A) represent significant difference within the same encapsulation property ($p < 0.05$).

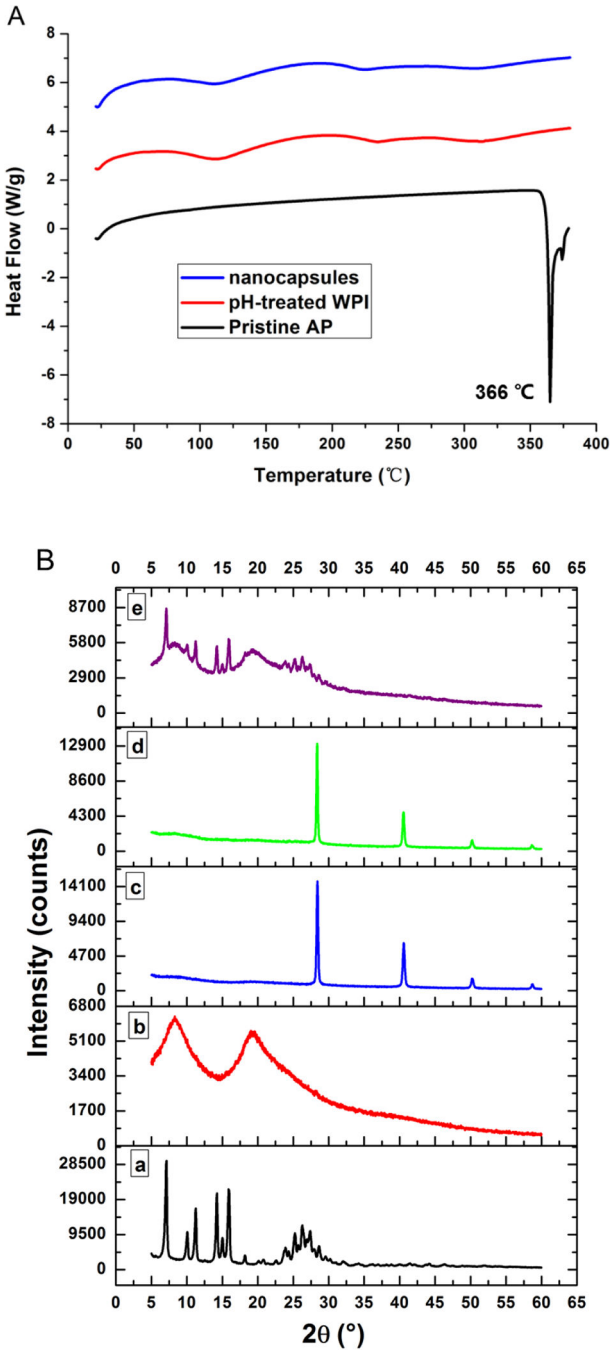

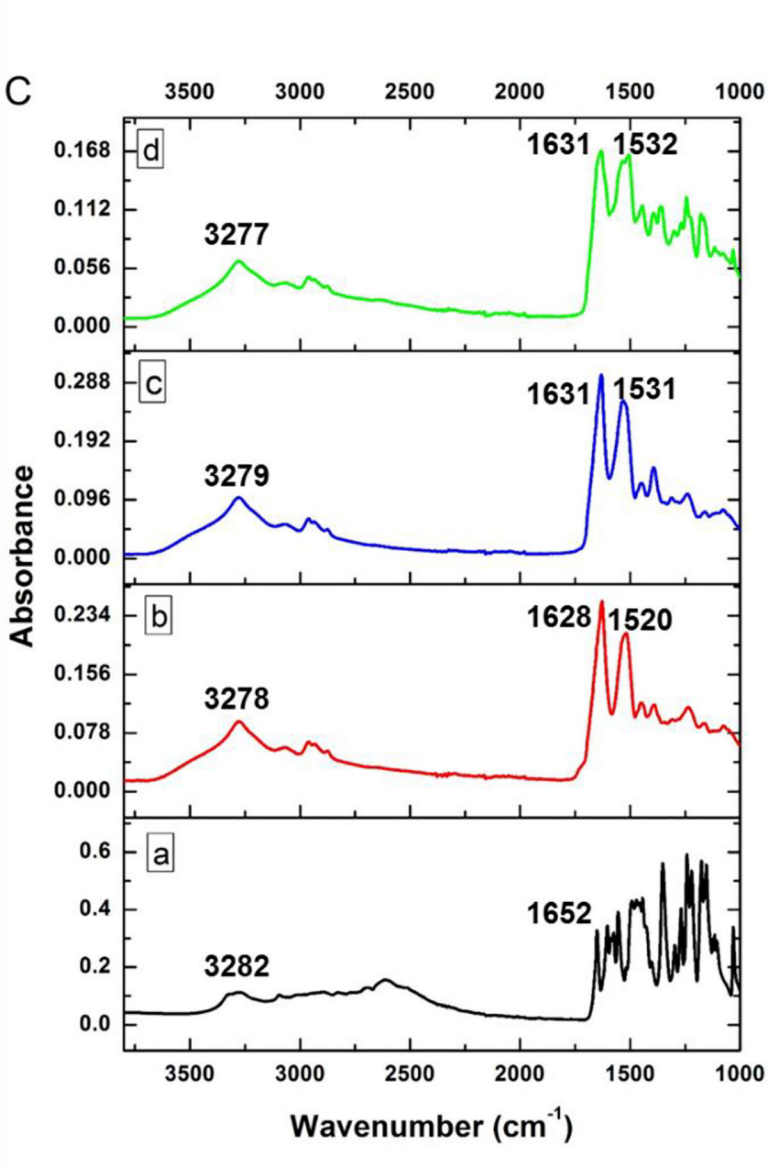


**Figure 2.**

(A) Comparison of DSC thermograms of pristine apigenin (AP), lyophilized WPI after the pH-cycle treatment (pH-treated WPI), and lyophilized powder of the nanodispersion prepared with 10.0 mg/mL WPI and 2.0 mg/mL AP using the pH-cycle (nanocapsules); (B) XRD patterns and (C) FTIR spectra of (a) pristine AP, (b) unprocessed WPI, (c) pH-treated WPI, (d) the nanocapsules, and (e) a physical mixture of pristine apigenin and unprocessed WPI.

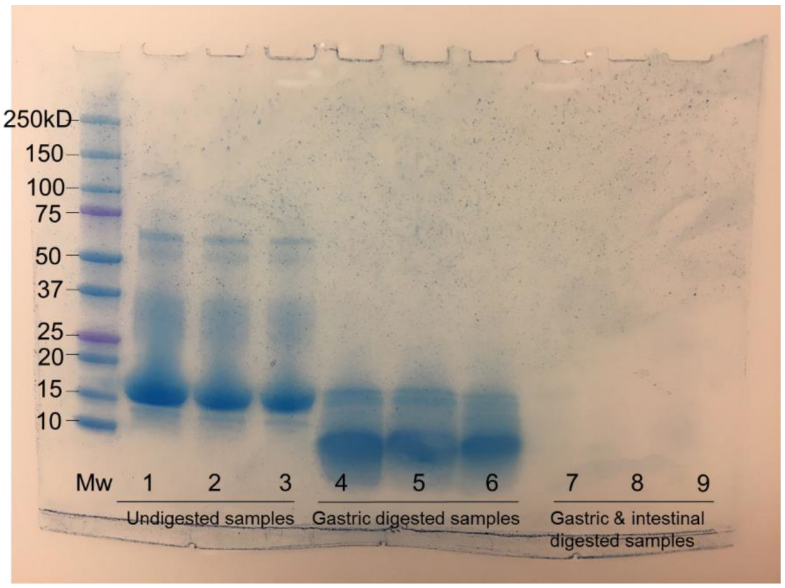


**Figure 3.**

SDS-PAGE analysis of, from left to right in each group, unprocessed WPI, WPI after the pH-cycle treatment, the nanodispersion prepared with 10.0 mg/mL WPI and 2 mg/mL apigenin before (samples 1–3) and after simulated gastric (samples 4–6) and sequential gastric and intestinal digestions (samples 7–9).

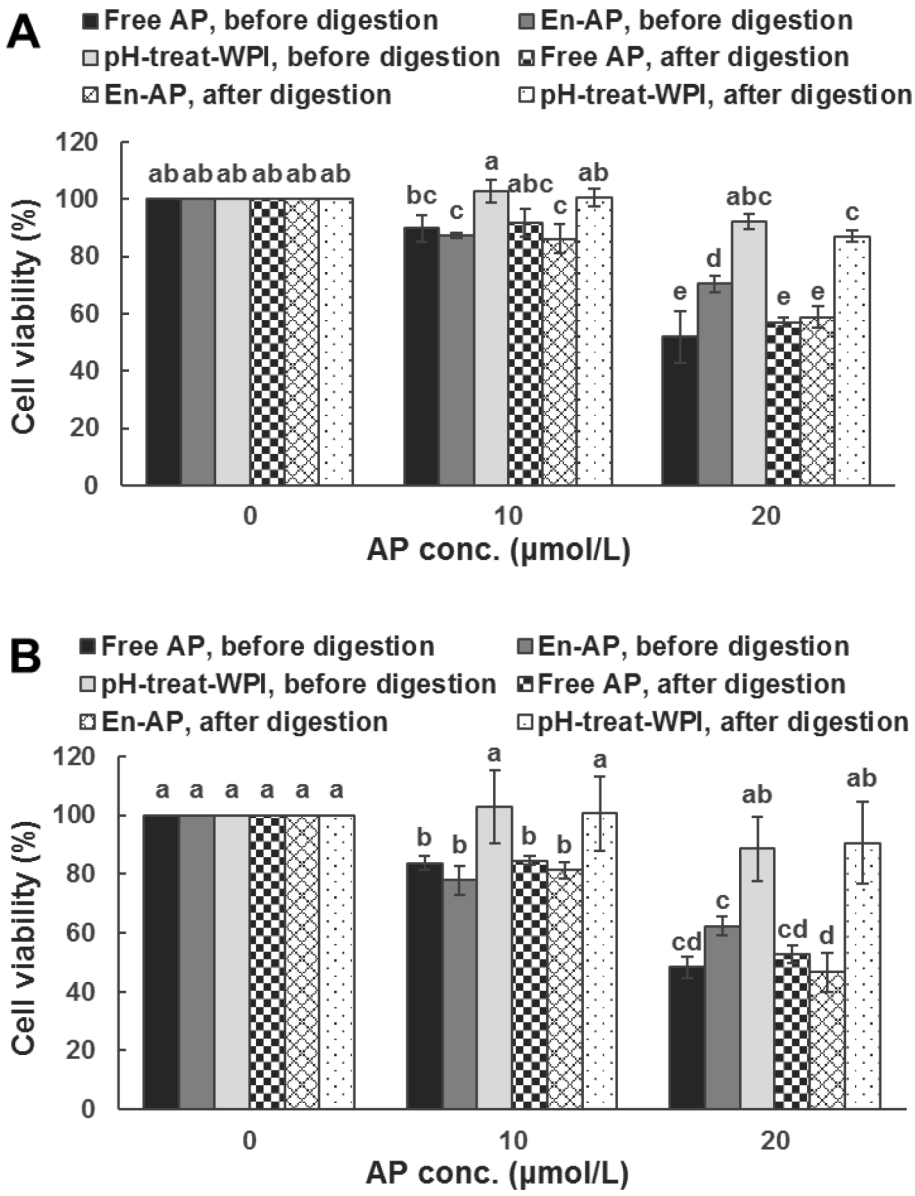


**Figure 4.**

The activity of 0 (medium only), 10, and 20 μmol/L apigenin (AP) pre-dissolved in DMSO (Free AP) or nanoencapsulated in WPI (En-AP), or WPI processed under the same pH cycle treatment (pH-treat-WPI), before and after simulated gastric and intestinal digestions, against the proliferation of (A) HCT-116 and (B) HT-29 colon cancer cells after 72-h incubation at 37 °C. The En-AP was prepared with 10.0 mg/mL WPI and 2 mg/mL AP using the pH-cycle. The pH-treat-WPI was prepared in the equivalent amount of that in En-AP. Error bars are SD (n = 3). Columns with different letters represented significant differences ($p < 0.05$).

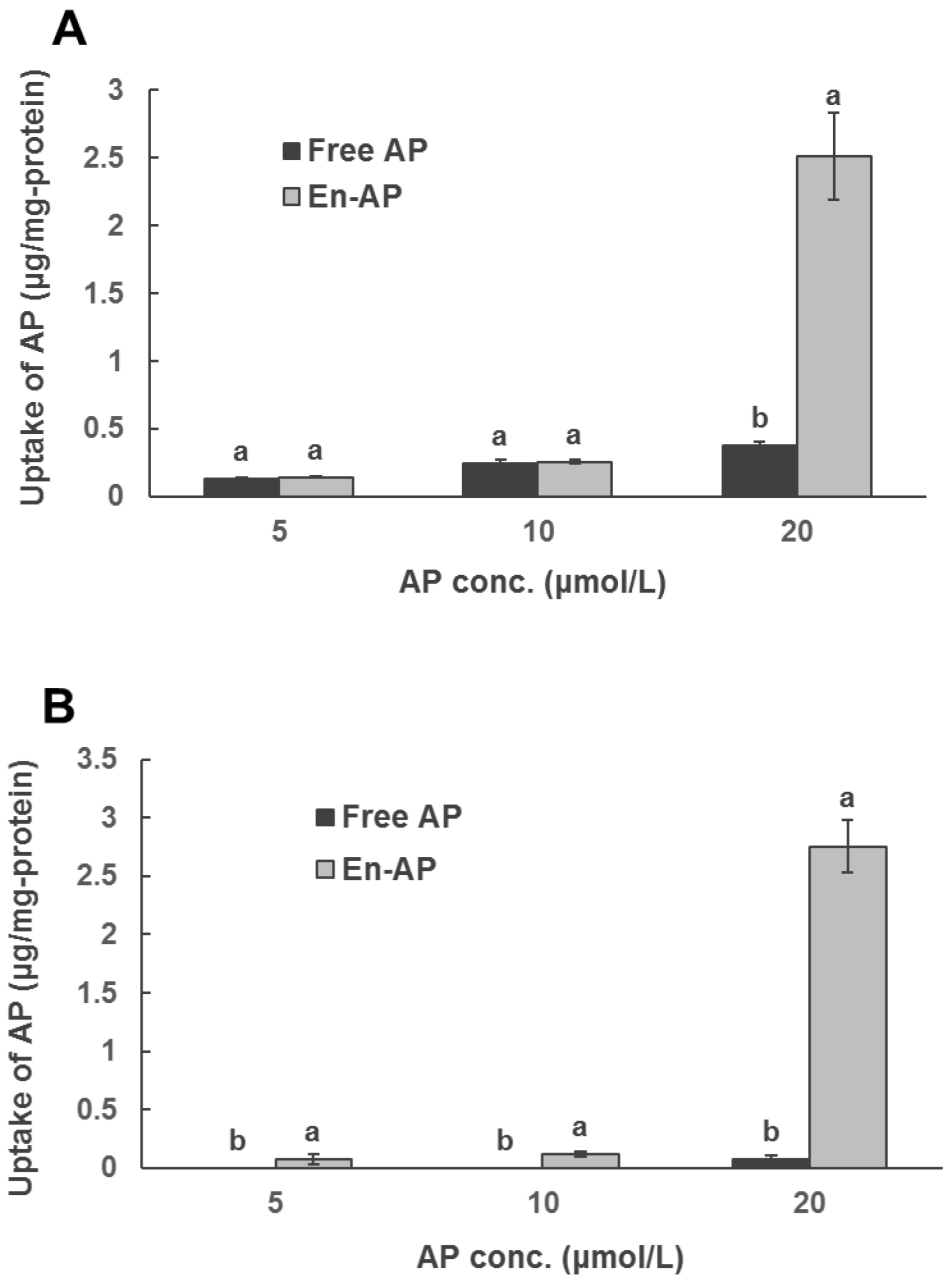


**Figure 5.**

Uptake of apigenin (AP) by (A) HCT-116 and (B) HT-29 colon cancer cells after treating with 5, 10, and 20 μmol/L of AP pre-dissolved in DMSO (Free AP) or nanoencapsulated in WPI (En-AP) for 24 h at 37 °C. The En-AP was prepared with 10.0 mg/mL WPI and 2 mg/mL AP using the pH-cycle. Error bars are SD (n = 3). Different letters above columns indicate significant difference between Free AP and En-AP at the same AP concentration ($p < 0.05$).

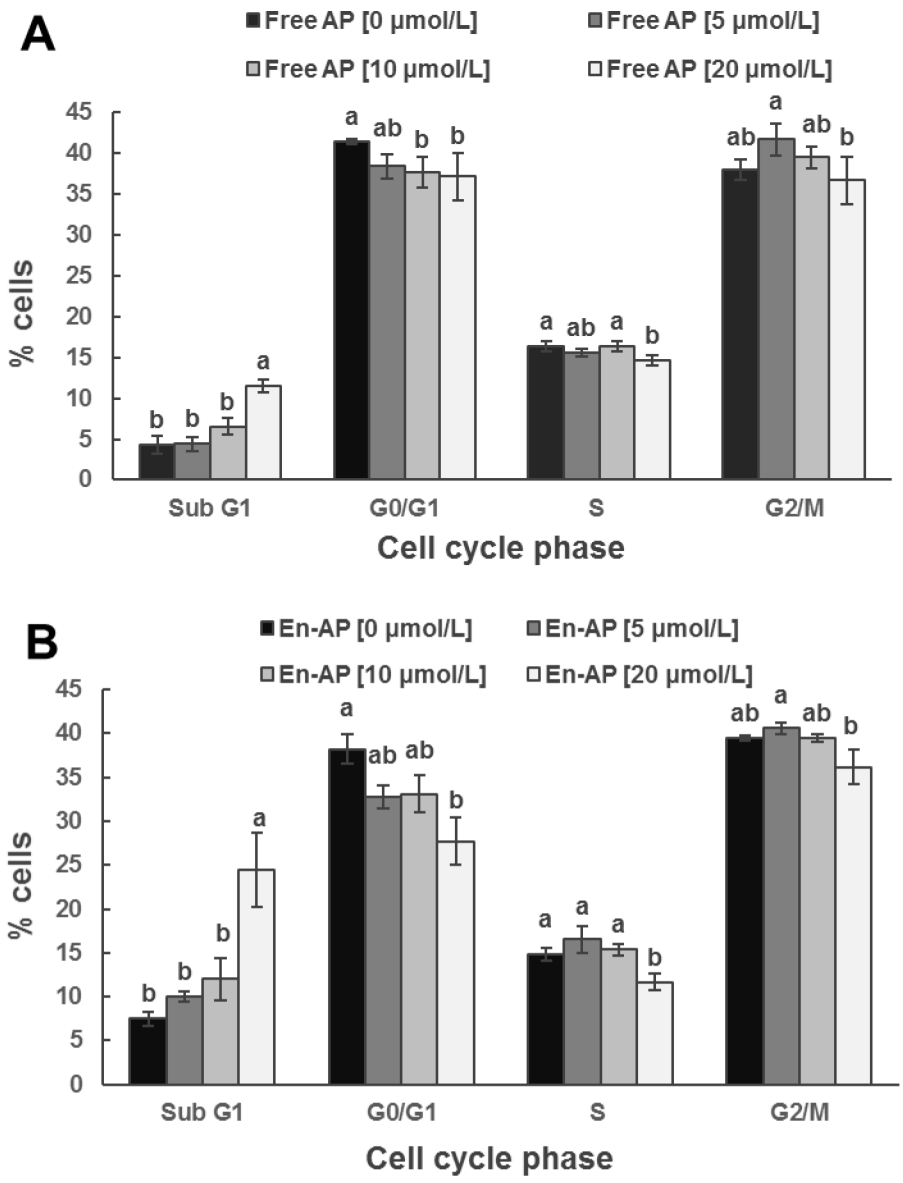


**Figure 6.**

Cell cycle distribution analyzed with flow cytometry for HCT-116 cell line after treatment with 0, 5, 10, and 20 μmol/L apigenin (AP) pre-dissolved in DMSO (Free AP, A) or nanoencapsulated in WPI (En-AP, B) for 24 h at 37 °C. The En-AP was prepared with 10.0 mg/mL WPI and 2 mg/mL AP using the pH-cycle. Error bars are SD (n = 3). Mean values with different letters within the same cell cycle phase are significantly different ($p < 0.05$).

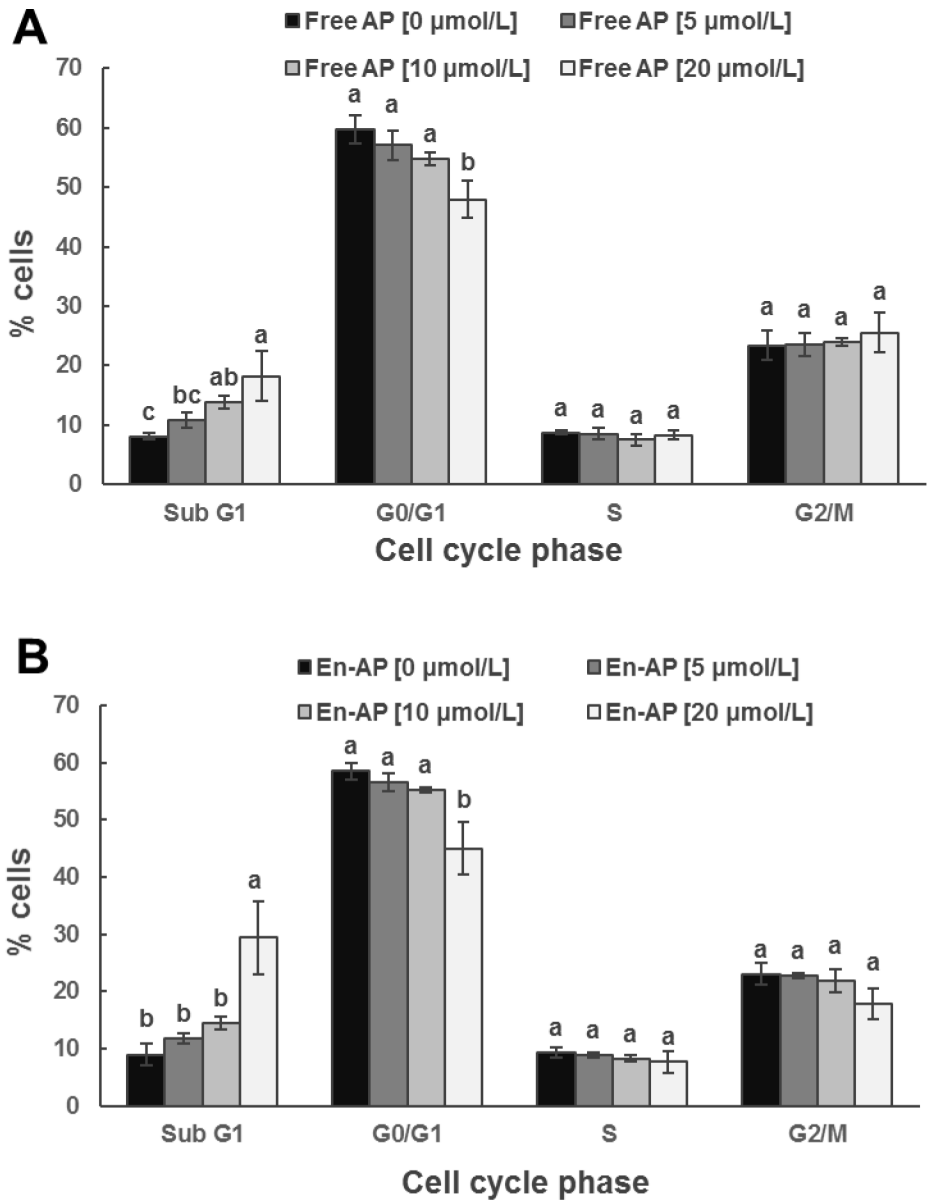


**Figure 7.**

Cell cycle distribution analyzed with flow cytometry for HT-29 cell line after treatment with 0, 5, 10, and 20 µmol/L apigenin (AP) pre-dissolved in DMSO (Free AP, A) or nanoencapsulated in WPI (En-AP, B) for 24 h at 37 °C. The En-AP was prepared with 10.0 mg/mL WPI and 2 mg/mL AP using the pH-cycle. Error bars are SD (n = 3). Mean values with different letters within the same cell cycle phase are significantly different ($p < 0.05$).

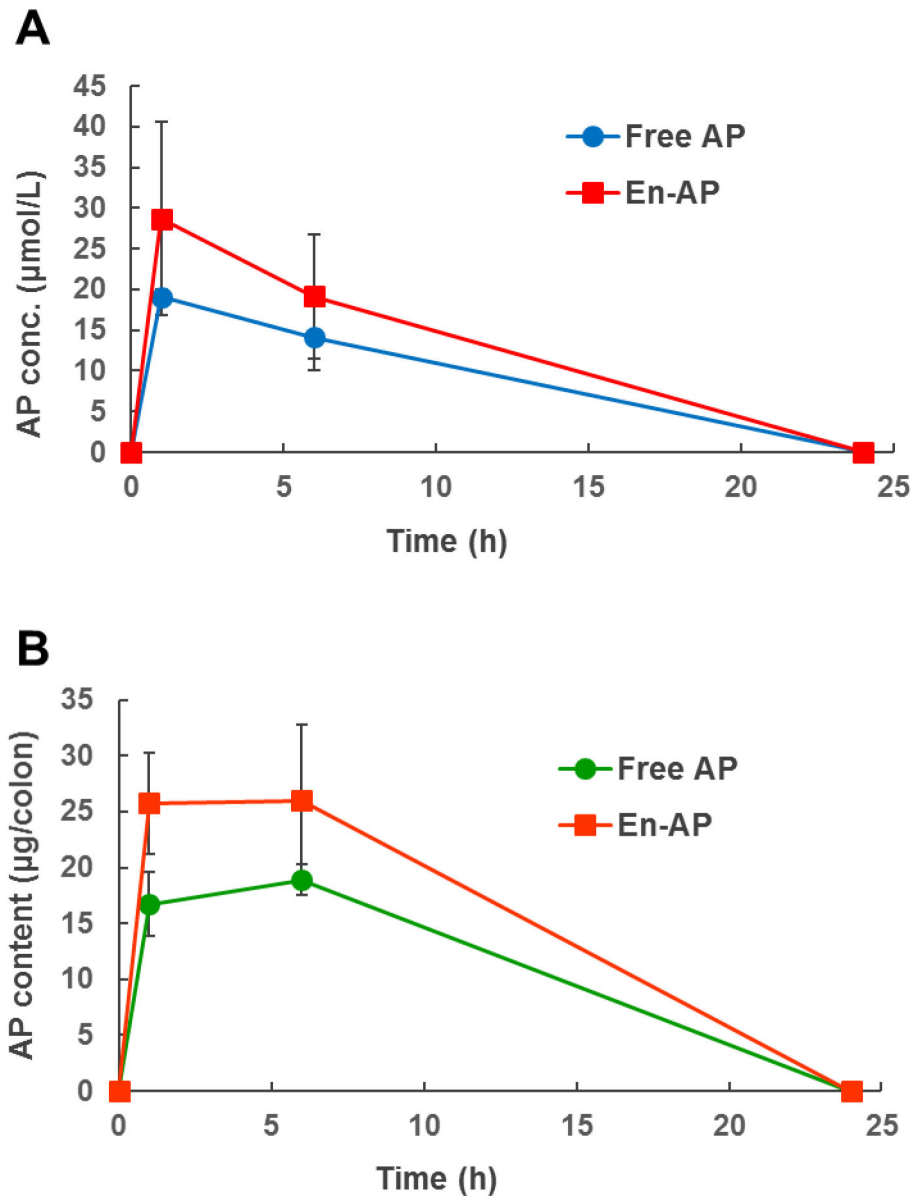


**Figure 8.**

The concentration of apigenin (AP) in the blood serum (A) and colon mucosa (B) of mice after oral gavage with 50 mg/kg-body mass of AP suspended in 5 mg/mL methylcellulose (Free AP) or nanoencapsulated in WPI (En-AP). Error bars are SD (n = 3 for 0 h time point, n = 4 for 1, 6, and 24 h time points).

**Table 1.**

Zeta-potential of pH 7.0 nanodispersions containing 10.0 mg/mL WPI and different concentrations of apigenin after the pH-cycle treatment.

| Apigenin (mg/mL) | Zeta-potential (mV)* |
|---|---|
| 0 | −20.43 ± 1.41 [a] |
| 0.6 | −20.10 ± 1.57 [a] |
| 1.0 | −20.50 ± 1.44 [a] |
| 1.5 | −21.53 ± 1.52 [a] |
| 2.0 | −21.60 ± 1.43 [a] |

*Numbers are mean ± SD (n = 3). The same superscript letters indicate no significant difference ($p > 0.05$).